

To be submitted to JCP 400 column lines or ~3.5 published pages (~6 MS Word pages)

## **On the importance of thermodynamic self-consistency for calculating stable clusters in hard-core double Yukawa fluids**

Authors: Jung Min Kim,<sup>1</sup> Ramón Castañeda-Priego,<sup>1,2</sup> Yun Liu,<sup>1,3</sup> Norman J. Wagner<sup>1,\*</sup>

<sup>1</sup>*Center for Neutron Science, Department of Chemical Engineering, University of Delaware, Newark, Delaware 19716, USA*

<sup>2</sup>*División de Ciencias e Ingenierías, Universidad de Guanajuato, Loma del Bosque 103, 37150 León, Mexico*

<sup>3</sup>*The NIST Center for Neutron Research, National Institute of Standards and Technology, Gaithersburg, Maryland 20899-6100, USA*

\*Corresponding author email: wagnernj@udel.edu

Phone: 302-831-8079

Fax: 302-831-1048

### *Abstract*

Understanding clustering of complex fluids is of interest in material science because the formation of aggregates in the suspension leads to changes in the material properties. Recently, using a mixed closure relation and a thermodynamic self-consistency criterion, Bomont et al. have shown the temperature dependence, at a fixed density, of the cluster formation in systems with short-range attractions and long-range repulsions which are modeled with the hard-core double Yukawa potential.<sup>1</sup> In this communication, we provide evidence that the cluster formation is a common behavior in systems with competitive interactions. In particular, we demonstrate that, based on the same thermodynamic self-consistency criterion, equally accurate structural information is obtained irrespective of the chosen mixed closure relation. Additionally, we explore the dependence of the clustering on the density and potential parameters. Our findings are corroborated with Monte Carlo computer simulations.

### *Introduction*

In prior work, the microstructure of equilibrium clustered structure of a fluid, characterized by hard-core double Yukawa (HCDY) potential with short-range attraction and long-range repulsion, was

accurately predicted by enforcing thermodynamic self-consistency (TSC) while mixing the hyper-netted chain (HNC) and Martynov-Sarkisov closures.<sup>1</sup> The study of such a fluid draws interest because it leads to a more in-depth understanding of globular protein solutions,<sup>2,3</sup> colloidal dispersions,<sup>4</sup> and food science.<sup>5</sup> However, as previously noted in a study of the square well (SW) potential, the range of parameters over which one can successfully achieve TSC depends on the choice of closure.<sup>6</sup> In our study, we demonstrate that the reversed hybridized mean spherical approximation (rHMSA) closure provides an equally accurate route to predicting equilibrium clustered fluids, as judged by Monte Carlo (MC) simulations.

A common criterion to obtain TSC is examining the isothermal compressibility,  $\chi$ , which, for pairwise additive potentials, can be calculated following the fluctuation  $\chi^{fluc}$ , and virial equation  $\chi^{vir}$  routes<sup>1,6-8</sup>,

$$\chi^{fluc} = \left(1 - \rho \int c(r) dr\right)^{-1} = kT \left(\frac{\partial \rho}{\partial p}\right) \Big|_T = \chi^{vir}, \quad (1)$$

where  $\rho$  is the particle number density,  $c(r)$  is the direct correlation function,  $kT$  is the thermal energy, and  $p$  is the pressure. Several studies have demonstrated that the TSC accompanied with various closures, including Rogers and Young and hybridized mean spherical approximation, can accurately predict structures of simple and/or complex fluids.<sup>8,9</sup>

In particular, the rHMSA closure, mixing of HNC and soft-core mean spherical approximation (SMSA), was successfully demonstrated for the attractive square well potential<sup>6</sup>. This closure reads as follows,

$$g(r) = e^{\frac{\Phi_1(r)}{kT}} \left(1 + \frac{1}{f(r)} \left[ e^{f(r) \left[ \gamma(r) - \frac{\Phi_2(r)}{kT} \right]} - 1 \right] \right), \quad (3)$$

$$f(r) = 1 - e^{-1/\alpha r}, \quad (4)$$

where  $\Phi_1(r)$  and  $\Phi_2(r)$  are the repulsive and attractive contributions, respectively, of the interparticle potential,  $f(r)$  is the bridge function,  $\gamma(r) = g(r) - c(r) - 1$ , and  $\alpha$  is the adjustable parameter to satisfy the TSC condition. Using three different closure relations, Bergenholtz et al. confirmed that the calculated structures are equivalent irrespective of the closure selected,<sup>6</sup> confirming that choosing an alternative closure in case of a solution convergence failure is valid.

## Methods

The DY pair interaction potential is one of the simplest continuous potentials to include both attractive and repulsive components. Here, we study the HCDY potential given by:

$$\Phi(r) = \begin{cases} \infty, & r^* \leq 1 \\ -K_1 \frac{\exp(-z_1(r^* - 1))}{r^*} + K_2 \frac{\exp(-z_2(r^* - 1))}{r^*}, & r^* > 1 \end{cases} \quad (5)$$

where  $K_1$ , and  $K_2$  denotes the magnitude of attraction, and repulsion, respectively,  $z_1$  and  $z_2$  denotes the range of attraction, and repulsion, respectively,  $r^*$  is the center-to-center separation distance normalized

by  $\sigma$ , the hard-core diameter. The reduced temperature is  $T^* = kT/\varepsilon$ , where  $\varepsilon = K_1 - K_2$  and the ratio between the factors is defined  $\xi = K_2/K_1$  hereafter.<sup>1</sup> The HCDY is advantageous in that repulsion and/or attraction can easily be varied or screened by assigning different parameters, which is useful to study many cases including protein stability and colloidal dispersions.<sup>2,10</sup>

Monte Carlo (MC) computer simulations were performed using a cubic box of length  $L^3 = N/\rho$  with  $N$  being the number of particles and following the Metropolis algorithm.<sup>11</sup> Simulations with  $N = 1000$ , 2197 and 4096 particles were carried out to analyze size effects. To present snapshots from the MC simulations, we only used results from 2197 particles case. We have chosen random initial configurations and the system was equilibrated during  $2 \times 10^7$  MC steps. The equilibration process was also monitored following the evolution of the total potential energy. Averages were performed during  $8 \times 10^7$  MC steps.  $S(q)$  was computed through the Fourier transform of the  $g(r)$  and directly from its definition, i.e.,  $S(q) = N^{-1}\langle\rho(\vec{q})\rho(-\vec{q})\rangle$ , where  $\rho(\vec{q})$  is the Fourier transform of the local density.<sup>12</sup> The latter procedure was computed over 2560  $\vec{q}$ -vectors with randomly chosen orientations. Both routes give us basically equivalent results. Moreover, structure functions are averaged over ten stochastic independent realizations to reduce the associate uncertainties.

### *Results and discussion*

We first study the clustering evolution as a function of temperature using the same potential parameters of Bomont et al.<sup>1</sup>,  $\xi=0.1$ ,  $z_1=10$ , and  $z_2=0.5$ , for direct comparison. Figure 1a shows the structure factor for  $T^*=11.1$ , 1.85, 0.85, 0.69, 0.62, and 0.46 at  $\varphi=0.15$ , where  $\varphi = \pi\sigma^3\rho/6$  is the so-called volume fraction. We here observe the following interesting features. Both closure relations and MC show that upon decreasing the temperature from  $T^*=11.1$  there is an increase in the peak at low- $q$ . This behavior in the  $S(q)$  has been interpreted as a signature of cluster formation. The growth of high intensity at low  $q$  is also experimentally observed in protein solutions studied by SANS.<sup>2,3</sup> However, according to the peak-position, the characteristic distance between clusters is about 4 particle diameters. This means that such clusters are composed of only a few numbers of particles. Moreover, in the whole temperature regime explored, the main peak is located around  $q^* \sim 2\pi$ , which means that the particle diameter is the most important length scale in the system. These features are indeed corroborated by the  $g(r)$ , see Figure 1b, whose contact value increases by lowering temperature, indicating that the pairing is the most favorable particle configuration. However, long-range order associated with the low- $q$  behavior in the  $S(q)$  is difficult to observe, since the  $g(r)$  decays rapidly to 1. Nonetheless, it should be noted that the peak associated with small clusters does not appear when the system is described by a hard-sphere interaction only<sup>13</sup>. Additionally, we observe that our closure relation and the one proposed by Bomont et al. (dashed line) give the same structural information and successfully reproduce the simulation data.

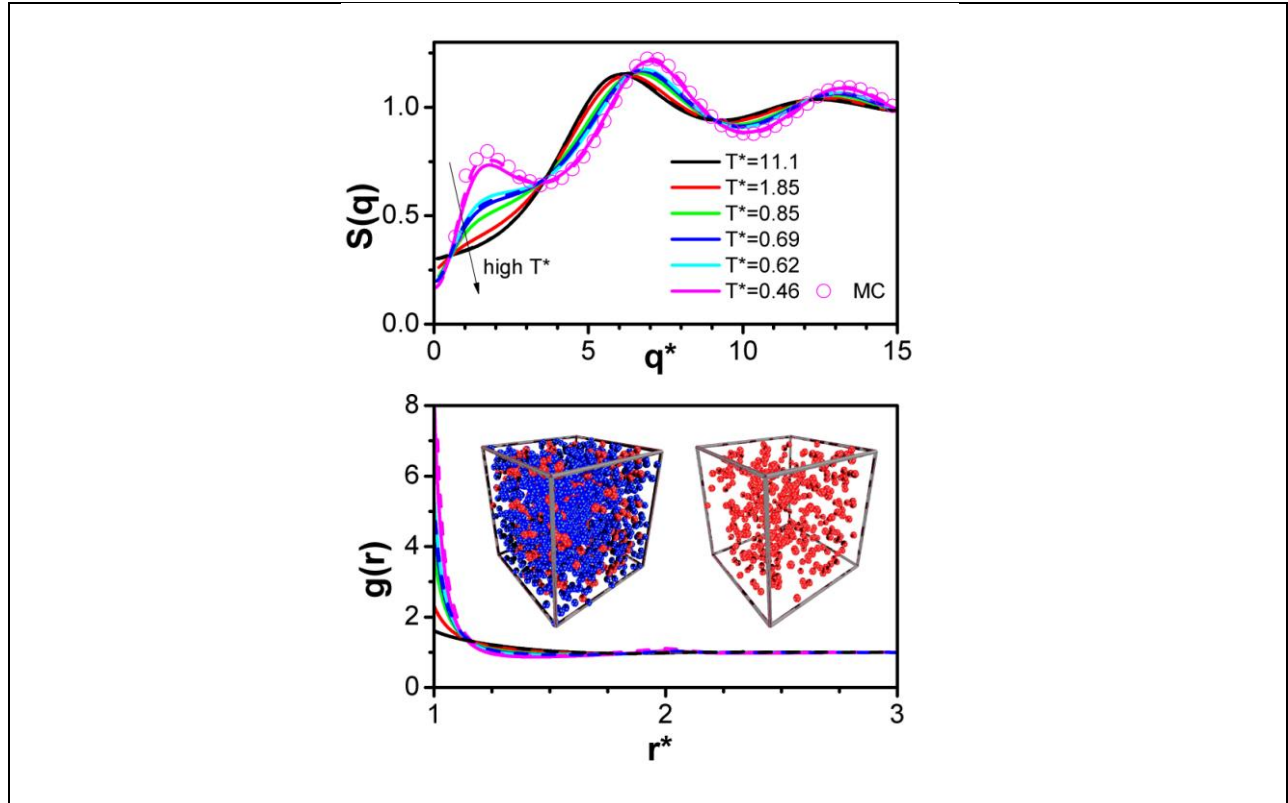


**Figure 1** A direct comparison of the two closures used by Bomont et al.<sup>1</sup> and in this study for  $\phi=0.15$ ,  $\xi=0.10$ ,  $z_1=10$ , and  $z_2=0.5$  at various  $T^*$ . The data of Bomont et al. and ours are represented by broken (digitized from the original paper), solid lines (calculated), and open circles (MC), respectively. In the simulations box, the blue and red particles indicate unclustered and clustered particles, respectively.  $q^*=q\sigma$  and  $r^*=r/\sigma$  hereafter.

We are now able to study the density dependence of the cluster formation. Figure 2b shows both  $S(q)$  and  $g(r)$  at a fixed temperature of  $T^*=0.46$ . Clearly, our closure relation accurately reproduces the full trend predicted in the MC simulation data, although slight differences at high densities are observed. Such differences can be attributed to the common phenomenon of closure relations underestimating structure of highly dense systems. However, in general, the following intriguing characteristics can be noticed. On one hand, we observe in the  $S(q)$  that a decreasing in  $\phi$  gives rise to a higher peak at low- $q$ . Note that increasing the  $\phi$  does not shift the location of either the cluster peak or the first neighbor correlation peak. This indicates that the cluster size and position are unrelated to  $\phi$ . On the other hand, the decreasing of the cluster-peak height with density means that the concentrations effects try to stabilize the system against the cluster formation. Additionally,  $g(r)$  shows a slight increase of the contact value with density and a peak located at  $r^*\sim 2$ . However, these features cannot be related with the cluster formation seen in the  $S(q)$ . Therefore, further analysis of the long-range behavior of the  $g(r)$  to clarify the physical mechanism of the clustering is evidently needed.<sup>14</sup>

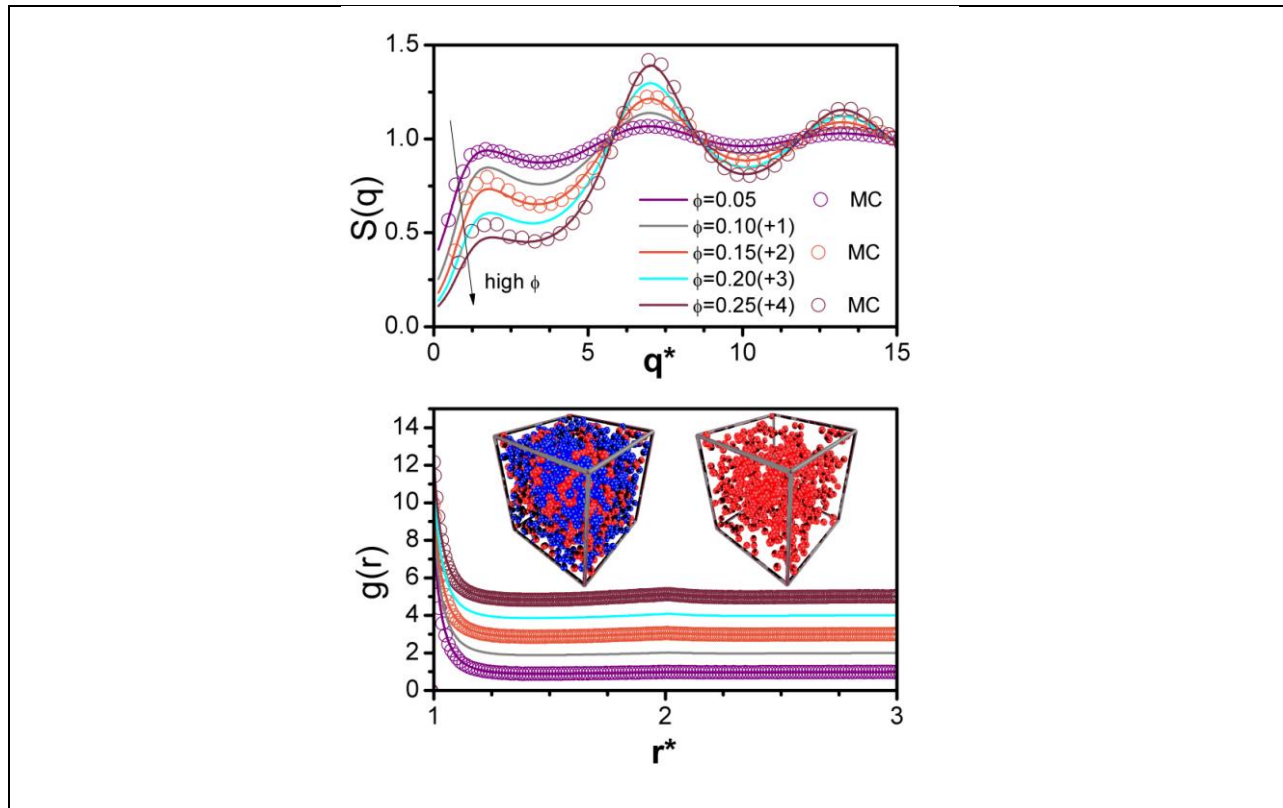


**Figure 2** Structures of liquid of different volume fractions with the double-Yukawa parameters  $\xi=0.10$ ,  $z_1=10$ , and  $z_2=0.5$  at  $T^*=0.46$ . The  $g(r)$  plot is progressively shifted by the respective factor for clarification.

Finally, we have studied the dependence of the structure on the screening parameters. We basically vary  $z_1$  or  $z_2$  to test the range of validity of the rHMSA closure. We observe that in both cases our approximation correctly reproduces the MC data. In particular, to test the effect of changing the range of repulsion,  $z_2$  is incrementally increased to 2 and 3 thereby decreasing the range of repulsion. Figure (3) shows that the peak height at low- $q$  decreases in the direction of increasing  $z_2$ . This change is believed to occur since the decreased range of repulsion hinders particles from aggregating with neighboring particles. The trend becomes more different when  $z_2=3$ . Also, decreasing  $z_1$  from 10 to 6 introduces more distinct cluster peaks while shifting the position of peak to lower  $q$ . Such peaks at low- $q$  seems to grow when the attractive Yukawa tail is sufficiently wide and/or deep to initiate the formation of clusters.<sup>10</sup>

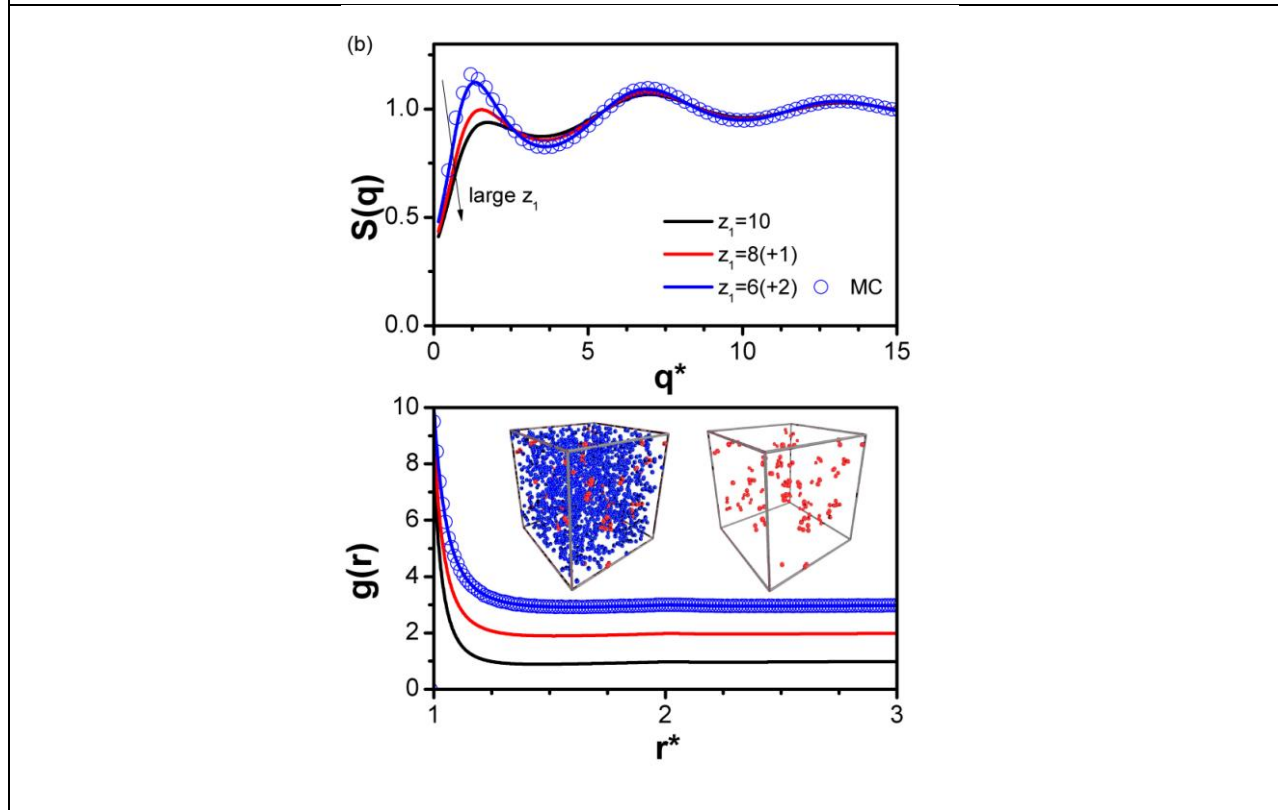
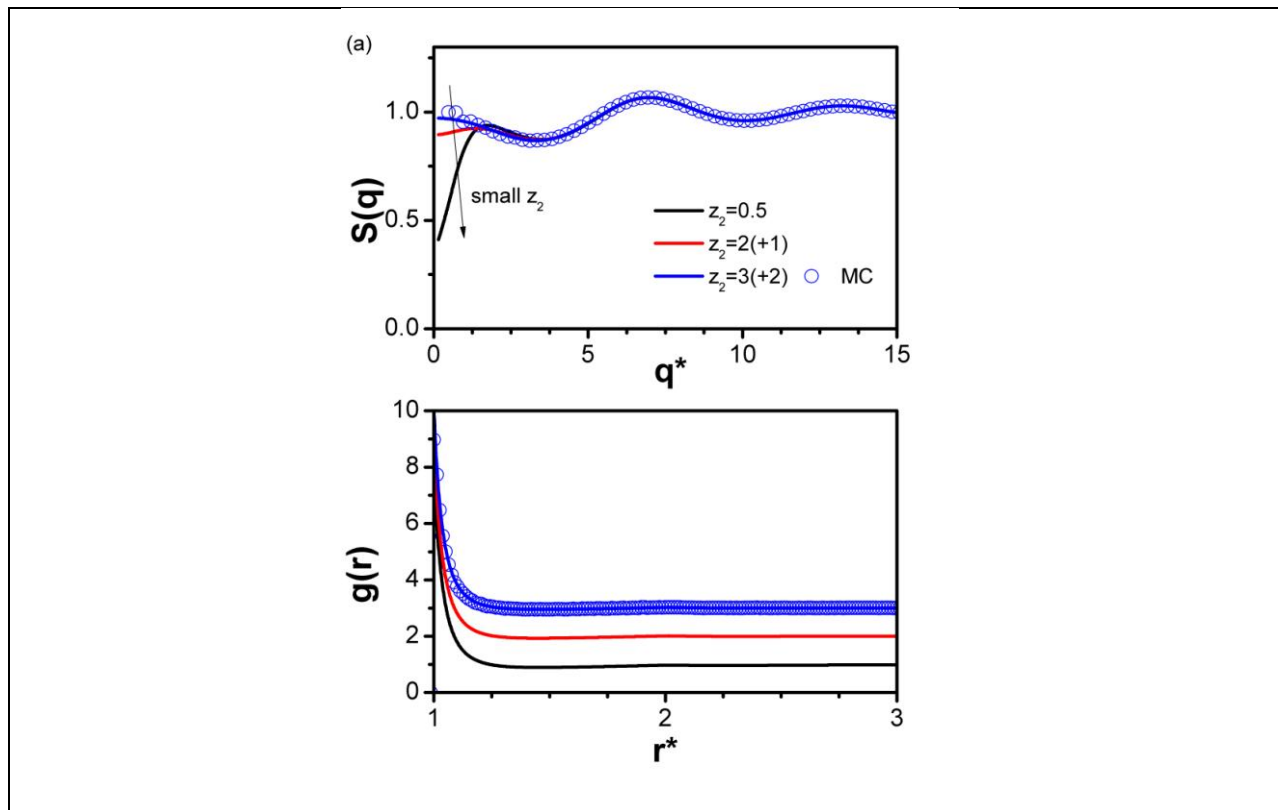


**Figure 3** Structures with (a) decreasing range of repulsion with  $z_2=0.5, 2,$  and while  $\varphi=0.05, \xi=0.10,$  and  $z_1=10$  at  $T^*=0.46,$  and (b) increasing range of attraction with  $z_1=10, 8,$  and  $6$  while  $\varphi=0.05, \xi=0.10,$  and  $z_2=0.5$  at  $T^*=0.46.$  The  $g(r)$  plots are shifted by the respective factor for clarification.

## Conclusions

We have shown that ensuring the condition of thermodynamic self-consistency is a robust method to accurately predicting fluid structures. We briefly probed structures at different conditions (temperature, density and potential parameters) using the hard-core double Yukawa fluid. We found that as long as the convergence of the solution is achieved, the choice of combination of closures does not greatly affect the final structural information. Therefore enforcing the thermodynamic self-consistency is more crucial to correctly describe structure than attempting to improve each ingredient closure. Additionally, our findings revealed that the physical mechanisms that lead to cluster formation in systems with competitive interactions are far to be well understood. However, our approach combined with computer simulations will allow elucidating the cluster formation in complex fluids.

## Acknowledgements

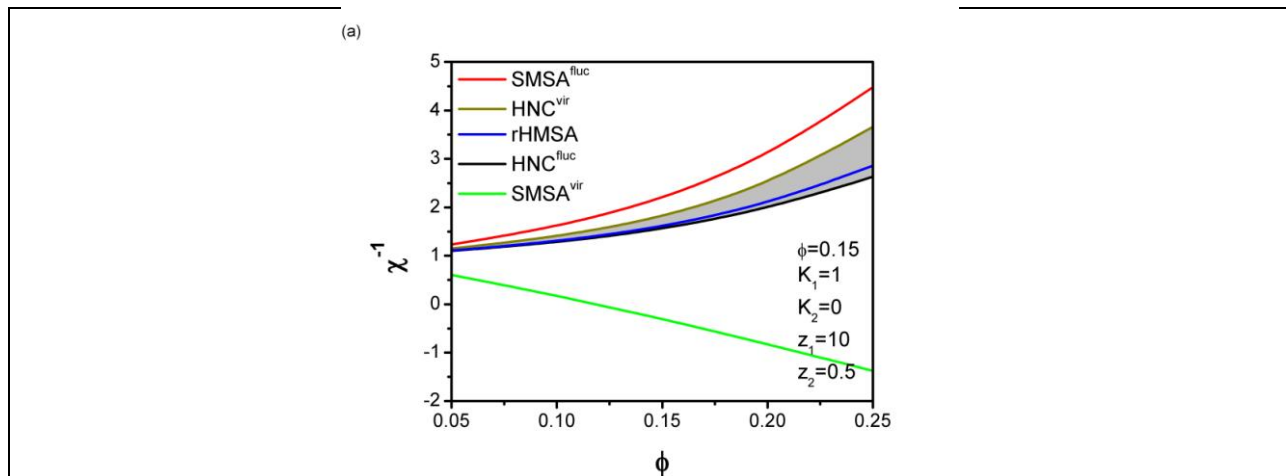
We gratefully acknowledge the funding for this research provided by Center for Neutron Science, funded by the National Institute of Standard and Technology under Cooperative Agreement # 70NANB7H6178 and by Conacyt-Mexico under the grant # 61418/2007 and 102339/2008.

## References

- <sup>1</sup> J. M. Bomont, J. L. Bretonnet, and D. Costa, *Journal of Chemical Physics* **132** (18), 9 (2010).
- <sup>2</sup> Y. Liu, W. R. Chen, and S. H. Chen, *Journal of Chemical Physics* **122** (4), 13 (2005).
- <sup>3</sup> A. Stradner, H. Sedgwick, F. Cardinaux, W. C. K. Poon, S. U. Egelhaaf, and P. Schurtenberger, *Nature* **432** (7016), 492 (2004).
- <sup>4</sup> P. J. Lu, E. Zaccarelli, F. Ciulla, A. B. Schofield, F. Sciortino, and D. A. Weitz, *Nature* **453** (7194), 499 (2008); M. D. Haw, M. Sievwright, W. C. K. Poon, and P. N. Pusey, *Physica a-Statistical Mechanics and Its Applications* **217** (3-4), 231 (1995).
- <sup>5</sup> R. Mezzenga, P. Schurtenberger, A. Burbidge, and M. Michel, *Nature Materials* **4** (10), 729 (2005).
- <sup>6</sup> J. Bergholtz, N. J. Wagner, and B. Daguanno, *Physical Review E* **53** (3), 2968 (1996).
- <sup>7</sup> D. A. McQuarrie, *Statistical mechanics*. (Harper & Row, New York, 1975).
- <sup>8</sup> F. J. Rogers and D. A. Young, *Physical Review A* **30** (2), 999 (1984); G. Zerah and J. P. Hansen, *Journal of Chemical Physics* **84** (4), 2336 (1986).
- <sup>9</sup> C. Caccamo, *Physics Reports-Review Section of Physics Letters* **274** (1-2), 1 (1996); U. Genz, B. Daguanno, J. Mewis, and R. Klein, *Langmuir* **10** (7), 2206 (1994); I. Guillen-Escamilla, M. Chavez-Paez, and R. Castaneda-Priego, *Journal of Physics-Condensed Matter* **19** (8), 14 (2007).

- 10 M. Broccio, D. Costa, Y. Liu, and S. H. Chen, *Journal of Chemical Physics* **124** (8), 9 (2006).
- 11 M. P. Allen and D. J. Tildesley, *Computer simulation of liquids*. (Clarendon Press; Oxford University Press, Oxford [England], New York, 1989).
- 12 J.-P. Hansen, *Theory of simple liquids*, 2nd ed. (Academic, London, 1986).
- 13 A. Cruz-Vera and J. N. Herrera, *Physica a-Statistical Mechanics and Its Applications* **387** (23), 5696 (2008).
- 14 S. Mossa, F. Sciortino, P. Tartaglia, and E. Zaccarelli, *Langmuir* **20** (24), 10756 (2004); T. Jiang and J. Z. Wu, *Physical Review E* **80** (2), 8 (2009); J. B. Caballero, A. M. Puertas, A. Fernandez-Barbero, and F. J. D. Nieves, *Colloids and Surfaces a-Physicochemical and Engineering Aspects* **270**, 285 (2005).

*Supplementary data*





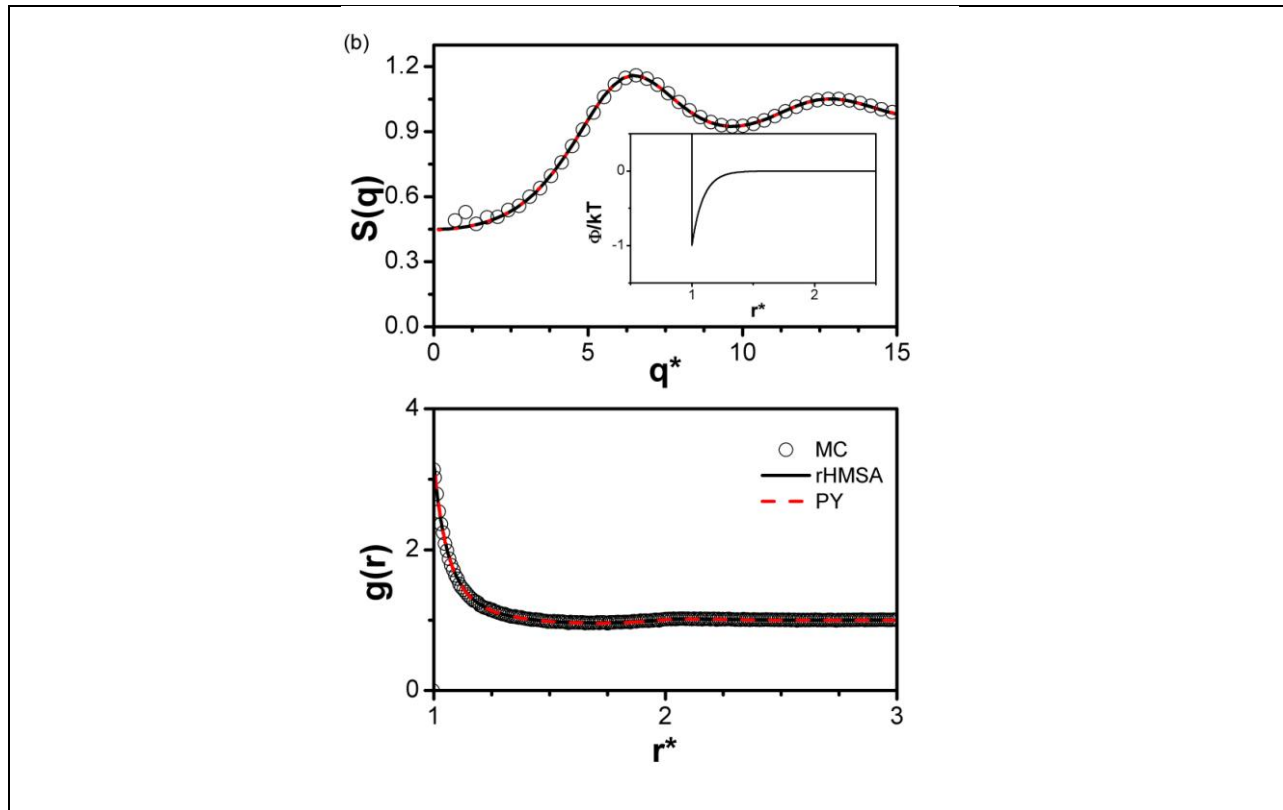


**Figure 4** (a) Anticipated inverse isothermal compressibility when each route is used. The shaded region indicates where the compressibility of the mixed closure will be located, as confirmed by the blue line. The HCDY parameters are  $K_1=1$ ,  $K_2=0$ ,  $z_1=10$ , and  $z_2=0.5$  with varying  $\phi$ . (b) Structure factor resulted from the attractive single-Yukawa with the given parameters using rHMSA (black solid), PY (red dash), and MC (black open circles). The three data sets are nearly indistinguishable. As  $q$  approaches 0,  $\chi$  is recovered by the relationship  $S(q \rightarrow 0)$ . The DY parameters are  $K_1=1$ ,  $K_2=0$ ,  $z_1=10$ , and  $z_2=0.5$  with  $\phi = 0.15$ .

Figure 4(a) describes that even though the  $\chi^{-1}$  calculated using each route may not be physically achievable, rHMSA leads to physically reasonable  $\chi^{-1}$ , which lies within the interpolated region between SMSA and HNC. Also, a good agreement between MC, rHMSA, and PY is observed in the structure and the radial distribution function. Therefore, we conclude that rHMSA works equally well for a continuous potential. The calculation was stopped at  $\phi=0.25$  due to limitations of the numerical analysis to obtain convergence; however, as the inverse isothermal compressibility lines indicate, the system is physically able to yield TSC convergence.